PB82-261413

Mathematical Model for Multicomponent Aerosol Formation and Growth in Plumes

California Inst. of Tech.
Pasadena

Prepared for

Environmental Sciences Research Lab.
Research Triangle Park, NC

21 Jan 81

U.S. Department of Commerce
National Technical Information Service
NTIS

aEH-6/17

TECHNICAL REPORT DATA
(Please read Instructions on the reverse before complet

1. REPORT NO.	2.	3.
EPA-600/J-81-581	JOURNAL ARTICLE	PB82-261413

4. TITLE AND SUBTITLE	5. REPORT DATE
MATHEMATICAL MODEL FOR MULTICOMPONENT AEROSOL FORMATION AND GROWTH IN PLUMES	6. PERFORMING ORGANIZATION CODE
7. AUTHOR(S) M. Bassett, F. Gelbard, and J.H. Seinfeld	8. PERFORMING ORGANIZATION REPORT NO.
9. PERFORMING ORGANIZATION NAME AND ADDRESS Department of Chemical Engineering California Institute of Technology Pasadena, California 91125	10. PROGRAM ELEMENT NO. CDTA1D/03-0559 (FY-82)
	11. CONTRACT/GRANT NO. 806844
12. SPONSORING AGENCY NAME AND ADDRESS Environmental Sciences Research Laboratory--RTP,NC Office of Research and Development U.S. Environmental Protection Agency Research Triangle Park, North Carolina 27711	13. TYPE OF REPORT AND PERIOD COVERED
	14. SPONSORING AGENCY CODE EPA/600/09

15. SUPPLEMENTARY NOTES
Reference: Atmospheric Environment, 15(10/11):2395-2406, 1981.

16. ABSTRACT

Description of the evolution of the size and chemical composition of aerosols in plumes is fundamental to the ability to predict visibility impairment. Previously, it has only been possible to predict changes in aerosol size distributions in plumes. In this work the first model for predicting both size and chemical composition evolution of plume aerosols is presented. Coagulation, homogeneous particle formation, heterogeneous condensation, and particle phase chemical equilibria and kinetics are explicitly included. The model is based on a sectional representation of the size-composition spectrum and computation is easy to implement. This model holds promise to be a standard component of all plume visibility calculations that require plume aerosol size and composition information.

17. KEY WORDS AND DOCUMENT ANALYSIS

a. DESCRIPTORS	b. IDENTIFIERS/OPEN ENDED TERMS	c. COSATI Field/Group

18. DISTRIBUTION STATEMENT	19. SECURITY CLASS *(This Report)*	21. NO. OF PAGES
RELEASE TO PUBLIC	UNCLASSIFIED	
	20. SECURITY CLASS *(This page)* UNCLASSIFIED	22. PRICE

EPA Form 2220-1 (Rev. 4-77) PREVIOUS EDITION IS OBSOLETE

REPRODUCED BY
NATIONAL TECHNICAL
INFORMATION SERVICE
U.S. DEPARTMENT OF COMMERCE
SPRINGFIELD, VA 22161

EPA-600/J-81-581
JOURNAL ARTICLE

Atmospheric Environment Vol. 15, No. 10/11, pp. 2395–2406, 1981
Printed in Great Britain.

MATHEMATICAL MODEL FOR MULTICOMPONENT AEROSOL FORMATION AND GROWTH IN PLUMES*

MARK BASSETT
Department of Chemical Engineering, California Institute of Technology, Pasadena, California 91125, U.S.A.

FRED GELBARD
Department of Chemical Engineering, Massachusetts Institute of Technology, Cambridge, Mass. 02139, U.S.A.

and

JOHN H. SEINFELD
Department of Chemical Engineering, California Institute of Technology, Pasadena, California 91125, U.S.A

(*First received* 10 *September* 1980 *and in final form* 21 *January* 1981)

Abstract—Description of the evolution of the size and chemical composition of aerosols in plumes is fundamental to the ability to predict visibility impairment. Previously it has only been possible to predict changes in aerosol size distributions in plumes. In this work the first model for predicting both size and chemical composition evolution of plume aerosols is presented. Coagulation, homogeneous particle formation, heterogeneous condensation, and particulate phase chemical equilibria and kinetics are explicitly included. The model is based on a sectional representation of the size-composition spectrum and computation is easy to implement. This model holds promise to be a standard component of all plume visibility calculations that require plume aerosol size and composition information.

NOMENCLATURE

a_i	activity of species i, mol (kg water)$^{-1}$ except a_w which is dimensionless
a_y, a_z	plume dispersion parameters
A	cross-sectional area of plume, m^2
b_y, b_z	plume dispersion parameters
c_i	molality of species i, mol (kg water)$^{-1}$
$\bar{C}[n, n]$	net rate of change of n by coagulation, $(\mu g)^{-2}$ m^{-3} s^{-1}
D	particle diameter, μm
D_l	particle diameter at the upper limit of section l, μm
D_{l-1}	particle diameter at the lower limit of section l, μm
$\mathcal{D}_B$	Brownian diffusivity, m^2 s^{-1}
$\mathcal{D}$	molecular diffusivity, m^2 s^{-1}
I_i	rate of change of component i in a particle due to condensation, g s^{-1}
$k_i(M)$	mass transfer coefficient of species i to a particle of mass M, μg s^{-1} atm^{-1}
k_g	first-order rate constant for gas-phase SO_2 oxidation, s^{-1}
$\overline{k_{li}}$	mean mass transfer coefficient for species i in section l, defined by (A.32), atm^{-1} s^{-1}
k_{pj}	mass transfer coefficient for species j to a particle with mass M_p defined by (A.33), atm^{-1} s^{-1}
K	equilibrium constant (see Table 1)
K_{ii}	turbulent eddy diffusivity in coordinate direction i, m^2 s^{-1}
Kn	Knudsen number, $2\lambda/D$
m	number of sections
m_i	mass of component i in a particle, μg
M	total mass in a particle, μg
M_i	molecular weight of species i, g mol^{-1}
n	size-composition density function, $(\mu g)^{-2}$ m^{-3}
N	total aerosol number density, m^{-3}
p_i	partial pressure of species i in gas phase, atm
p_{ie}	partial pressure of species i in gas phase in equilibrium with the particle composition, atm
p_{ile}	partial pressure of species i in gas phase in equilibrium with the mean particle composition of section l, atm
q_l	average mass concentration in section l, μg m^{-3}
Q_l	total aerosol mass in section l, μg m^{-3}
Q_{li}	total aerosol mass of species i in section l, μg m^{-3}
r_{li}	rate constant for species i in section l, from $(dm_i/dt) = r_{li}M$, s^{-1}
R_i	rate of change of component i in a particle due to intra-particle chemical reaction, μg s^{-1}
R.H.	relative humidity, %
s	number of components in the particulate phase
S	rate of introduction of particles, $(\mu g)^{-2}$ m^{-3} s^{-1}
t	time, sec
t'	plume travel time, $x_1/\bar{u}_1$, s
u	velocity of air (u_1, u_2, u_3), m s^{-1}
$\hat{u}$	generalized velocity in phase space
w_s	setting velocity of a particle, m s^{-1}
x	spatial position vector (x_1, x_2, x_3), m
y_i	gas-phase mixing ratio of species i, ppm
z	charge on a species

Greek

α_i	coefficients in heterogeneous rate expression, $i = 1, 2, 3$
$\overline{\beta_{ijk}}$	intra-sectional coagulation coefficient, defined by (A.34), m^3 μg^{-1} s^{-1}
$\overline{\beta_{ij}}$	inter-sectional coagulation coefficient, defined by (A.35), m^3 μg^{-1} s^{-1}

* Paper presented at the Symposium on Plumes and Visibility: Measurements and Model Components. Grand Canyon, Arizona, U.S.A. 10–14 November 1980.

$\beta(U, M)$	coagulation coefficient for particle with masses U and M, $m^3 s^{-1}$
γ_z	activity coefficient for species with charge z
Δ_i	$\ln(M_i/M_{i-1})$
ε	fractional error
ζ	ratio of the mass of sulfate to the total mass of a particle
θ	conditional function used in (A.26)
λ	mean free path of air, μm
σ_y, σ_z	standard deviations of plume dimensions, m
χ	total molality of HSO_4^-, SO_4^{2-}, and Mn^{2+}, mol(kg water)$^{-1}$
ω	$(1.333 + 0.71 Kn^{-1})/(1 + Kn^{-1})$

Symbols

$\bar{}$	time average (except for $\bar{x}_{ij}$ which is a sectional average)
$'$	fluctuating quantity
$\langle\ \rangle$	plume cross-sectional average

1. INTRODUCTION

A mathematical model for visibility impairment from either plume blight or regional haze must contain three ingredients: (1) a treatment of the advection and diffusion of gases and particles; (2) a routine for calculating visual range given the atmospheric gas and aerosol concentrations, viewing angle, solar angle, etc.; and (3) a description of the gas–particle dynamics, including the evolution of aerosol size and chemical composition. Items (1) and (2) have received considerable attention in visibility and other models. The major missing aspect in all current visibility models is a detailed treatment of the gas–aerosol dynamics. What is usually done is to specify the aerosol characteristics on the basis of empirical observations rather than to simulate them from first principles. However this approach provides little insight into the governing mechanisms. The object of this paper is to develop and present a model based on first principles for the dynamics of atmospheric aerosol size and chemical composition and to apply the model to predict aerosol size and composition as a function of downwind distance in a plume in which SO_2 is being converted homogeneously and heterogeneously to sulfate aerosol.

Prediction of the effect of changes in primary gaseous and particulate emission levels on particulate air quality necessitates the development of mathematical models that include aerosol processes and gas-to-particle conversion. Aerosols that do not change properties once in the atmosphere may be treated from a modeling point of view as inert gaseous species, with due attention to wet and dry deposition. As long as the aerosols do not interact or grow in the atmosphere, their size distribution is altered only through these removal processes which may be accounted for in a straightforward manner. However, most atmospheric aerosols do interact and grow by gas-to-particle conversion and thus more sophisticated approaches must be adopted. The prediction of both aerosol size and composition is the ultimate goal of aerosol modeling efforts and is the issue addressed in this paper.

Although there exists a large number of reported ambient aerosol size distributions (Willeke *et al.*, 1974; Willeke and Whitby, 1975; Hidy, 1975; Whitby, 1978) as well as efforts to characterize various atmospheric aerosol size distributions by empirical relationships, such as by sums of log-normal distributions, observed atmospheric aerosol size spectra and aerosol compositions have not been predicted *a priori*. The reason for this is twofold. First, until recently it has not been possible to solve the general dynamic equation governing a coagulating multicomponent aerosol, even without considering gas-to-particle conversion, sources, or removal mechanisms (Gelbard and Seinfeld, 1980). Second, the size distribution and chemical composition of typical primary aerosols are not adequately known, and the major secondary species and their chemical and physical routes of incorporation into particles have yet to be completely identified. Even though not enough is known about the chemistry and physics of individual particles to support predictions of the evolution of complex atmospheric aerosols, it is now possible to attempt to explain the nature of atmospheric aerosol size distributions and to begin to develop mathematical models capable of relating primary gaseous and particulate emissions to ambient aerosol size and chemical composition distributions. The model presented in this work will predict aerosol size distribution and composition given inputs of gas- and particulate-phase chemistry and primary particle emissions. Based on the model, light scattering calculations which incorporate both particle size and chemical composition effects can be used for visibility predictions.

In section 2 we present the basic equations governing the multicomponent sectional plume model. The detailed derivation of the model is given in Appendix A2. The discussion in Section 2 is aimed at describing the essential assumptions needed to obtain the model and describing the physical significance of each of its terms. In essence, the model represents a temporally (turbulent), spatially, and size/composition-averaged form of the fundamental aerosol conservation equation. Section 3 is devoted to an application of the model to a plume aerosol. All phenomena that might be expected to be important in a plume are included in the example, primarily as a means of illustrating the features of the model. The case considered consists of a power plant plume aerosol containing an aqueous solution of $MnSO_4$ that evolves due to absorption of SO_2 followed by liquid-phase catalytic oxidation, coagulation, and gas-to-particle conversion of sulfuric acid vapor generated by gas-phase oxidation of SO_2.

2. MULTICOMPONENT AEROSOL DYNAMICS

Gelbard and Seinfeld (1980) have developed a general method for simulating the evolution of the distribution of chemical species with respect to aerosol particle size. The physical phenomena included are: (1)

coagulation; (2) intra-particle chemical reaction; (3) gas-to-particle conversion and (4) particle sources and removal mechanisms. Thus, for the first time a technique is available for computation of not only the evolving size distribution but also the variation of chemical composition with particle size. In Appendix A1 and A2, a detailed extension of the multicomponent sectional technique developed by Gelbard and Seinfeld (1980) is presented for a plume aerosol. Therefore, only an outline of the logic used to develop the plume model follows.

Consider for the moment a spatially homogeneous aerosol in which particle size is characterized by a single variable M, particle mass, which is conserved during coagulation and intra-particle chemical reactions. By dividing the entire particle size domain into m contiguous arbitrarily sized sections and defining Q_l as the total mass of aerosol per unit volume of fluid in section l at time t we have, by definition,

$$Q_l = \sum_{i=1}^{s} Q_{il}, \tag{1}$$

where Q_{il} is the mass of component i in section l, and s is the total number of components in the particulate phase. M_{l-1} and M_l will denote the masses of the smallest and largest particles, respectively, in section l. Note that M_0 is arbitrary and the upper bound of section $l-1$ is equal to the lower bound of section l for $l = 2, 3, \ldots, m$. The model derived in this work describes Q_{il} in a plume.

A detailed model of Q_{il} as a three-dimensional, time-dependent function would clearly be the most comprehensive approach available. However, such a model would probably be of limited use due to: (1) the scarcity of detailed aerosol and meteorological data needed to justify such a complicated approach and (2) the excessive computational requirements of such a detailed model. Furthermore, much insight can be gained by using a steady state, spatially and temporally averaged plume model that does not have the above shortcomings. Thus, in the proposed one-dimensional, steady state model Q_{il} is determined in an expanding puff traveling with a mean wind velocity.

The summary of the approximations used to obtain the model is:

1. Neglect Brownian diffusion for bulk transport of particles.
2. Time-average and neglect terms containing temporal fluctuations for coagulation and condensation.
3. Spatially average in the x_2–x_3 plane for a plume traveling in the x_1-direction.
4. All particles within a section are approximated as being uniformly distributed with respect to the logarithm of $(D/1\ \mu m)$ (where D is the particle diameter).
5. All particles within a section are approximated as being of uniform composition in component i ($i = 1, 2, \ldots, s$) given by Q_{il}/Q_l.

Note that by temporally and spatially averaging, the only coordinate upon which Q_{il} depends is x_1, the distance downwind from the plume source. Therefore, one can define "a plume time" $t' = x_1/\bar{u}_1$, where $\bar{u}_1$ is the mean speed in the x_1-direction. The set of ms differential equations governing Q_{il} is*

$$\frac{dQ_{il}}{dt} = \underbrace{\left[\overline{k_{il}}(\langle \bar{p}_i \rangle - p_{ilo}) + r_{il}\right]Q_l}_{\text{A}}$$

$$\underbrace{-\left[\sum_{j=1}^{s}\left(k_{ej}(\langle \bar{p}_i \rangle - p_{ilo}) + r_{ij}\Delta_q^{-1}\right)Q_{qi}\right]\Bigg|_{q=l-1}^{q=l}}_{\text{B}}$$

$$\underbrace{+\tfrac{1}{2}\sum_{j=1}^{l}\sum_{k=1}^{l}\left({}^1\overline{\beta}_{ijk}\,Q_{ji}\,Q_k + {}^1\overline{\beta}_{ikj}\,Q_{ki}\,Q_j\right)}_{\text{C}}$$

$$\underbrace{-Q_{il}\sum_{j=1}^{m}{}^2\overline{\beta}_{ij}\,Q_j}_{\text{D}} \underbrace{-Q_{il}\frac{1}{A}\frac{dA}{dt'}}_{\text{E}} + \underbrace{\langle \overline{S}_{il} \rangle}_{\text{F}} \tag{2}$$

$$l = 1, 2, \ldots, m$$
$$i = 1, 2, \ldots, s.$$

Term A represents the net rate of addition of the i-th component to section l by the heterogeneous condensation of vapor molecules onto particles within section l and by aerosol-phase chemical reactions occurring in particles of section l. Term B represents the net rate of change of Q_{il} by condensation and aerosol-phase chemical reaction due to the growth of particles in section l-1 into section l and to the growth of particles in section l into section $l+1$. As a particle grows by condensation of vapor or as a result of chemical reactions, it may eventually leave its section, while, at the same time, some of those in the lower section may grow into that section. Thus, together, terms A and B represent the net rate of change of component i in section l from intra-section processes and growth between sections.

Terms C and D represent the effects of coagulation. Term C represents the rate of addition of particles to section l resulting from all collisions involving particles in sections lower than and including section l itself. Term D accounts for the rate of removal of component i from section l due to the collision of particles in section l with those of all other sections.

Term E represents the effect of dilution of the plume. Finally, term F represents the rate of addition of mass of component i to section l by sources. In the plume situation, the original source of particles appears as an initial condition on (2),

$$Q_{il}(t'_o) = Q^0_{il}, \tag{3}$$

and $\langle \overline{S}_{il} \rangle = 0$ for all sections l, except possibly for $l = 1$ if new particle formation by nucleation is occurring as a source of fresh particles into the first section. (It is assumed by this statement that if homogeneous

* All symbols are defined in Appendixes, A.1 and A.2 and in the Nomenclature section.

nucleation is occurring, the particles so formed would be of a size such that they would fall within the first section. This assumption is, of course, not necessary; fresh particles can be added to any section through specification of $\langle \overline{S}_{ii} \rangle$.)

Equation (2) is the result of a careful accounting of all aerosol processes that add or remove mass of a component from a section on the particle size domain. The particular form of (2) is that for the plume cross-section averaged sectional concentrations, as indicated by the spatial averaging brackets, $\langle\ \rangle$. The coefficients $\overline{k}_{ii}$ and k_{pj} are determined based on the gas-to-particle conversion processes occurring, whereas r_{ii} depends on heterogeneous reactions that are taking place. The term $A^{-1}\,dA/dt$ is determined by the rate of expansion of the plume.

To illustrate the application of the multicomponent sectional model we now consider predicting the evolution of a power plant plume aerosol. The example we will present is, for the most part, hypothetical. With the introduction of a new model such as that just described it is important that the first application be an example that is carefully defined and for which the calculations may be repeated by others interested in using the model. In the example that follows we have endeavored to include all important phenomena that influence a plume aerosol. The initial aerosol size distribution is taken from the plume field data reported by Eltgroth and Hobbs (1979). The composition of the initial aerosol is assumed to be an aqueous $MnSO_4$ solution, for which an empirical expression is available for the rate of oxidation of dissolved SO_2 to sulfate. All parameters that need to be specified are set at atmospherically relevant values. Thus, while the calculation does not correspond to an actual plume, each element of the model is treated realistically so that application to an actual field situation in which the particles consist of aqueous solutions follows from that presented here.

3. APPLICATION TO POWER PLANT PLUME AEROSOL

We consider the problem of predicting the evolution of the aerosol size and composition distribution in a power plant plume. Upon emission from the stack, we assume that the primary aerosol consists of an aqueous $MnSO_4$ solution and that the gas contains SO_2. As the plume is carried downwind and disperses, the SO_2 is both absorbed by the plume aerosol particles and converted to H_2SO_4 vapor by gas-phase chemistry. In the particles, the dissolved SO_2 is catalytically oxidized to sulfate (SO_4^{2-}), while, at the same time, the sulfuric acid vapor molecules from the vapor phase SO_2 oxidation are absorbed by the particles. Particle growth occurs due to the water vapor pressure lowering effect of the sulfate formed in the particles. The ambient relative humidity and temperature are assumed to be known, as is the background concentration of NH_3. It is desired to predict the distribution of all the dissolved aerosol species with particle size as a function of downwind distance.

Although the specific conditions of our example do not correpond to those of a particular plume, they have been chosen to reflect as closely as possible the situation in an actual plume. Only the gas-phase conversion of SO_2 to H_2SO_4 will not be treated in detail, as this step is only of peripheral interest to the model. In particular, the gas-phase oxidation of SO_2 is treated as first-order in SO_2, with the rate of formation of H_2SO_4 vapor given by

$$\frac{dp_{H_2SO_4}}{dt'} = k_g p_{SO_2}. \tag{4}$$

It is necessary to specify the following parameters to exercise the model: $\overline{k}_{ii}$ = the section average coefficient for gas-to-particle conversion of component i; $\langle \bar{p}_i \rangle$ = the mean partial pressure of each condensing component; p_{ii_0} = the partial pressure of component i in equilibrium with the particles in section i; r_{ii} = the rate constant for production of component i by intraparticle chemical reaction in section i; ${}^1\overline{\beta}_{ijk}$, ${}^2\overline{\beta}_{ij}$ = the sectional coagulation coefficients; and $(1/A)\,(dA/dt')$ = the rate of plume expansion. In addition, the number of species, s, and the number m and locations of the sections must be specified.

Physically, the plume aerosol consists of aqueous droplets containing $MnSO_4$, in the amount specified as initially present, together with the other components that result from the dissolution of SO_2, NH_3 and H_2SO_4 in the droplets. The time needed for equilibrium to be established between the gas and liquid phases is much shorter than that for coagulation or formation of sulfuric acid. Therefore, all the liquid-phase compositions, except those of Mn^{2+} and SO_4^{2-}, are determined by equilibrium with the gas phase. That is, once the concentrations of Mn^{2+} and SO_4^{2-} are specified, the entire composition of the particle is fixed through chemical equilibrium. As a result, Mn^{2+} and SO_4^{2-} are the only two components for which the multicomponent sectional equations are needed, i.e. $s=2$. The calculation proceeds as if the particles consist solely of Mn^{2+} and SO_4^{2-}, although the particles are considerably more complex, and the parameters listed above must be determined on the basis of the actual particle composition. The dependent variables in the model are Q_{i1} and Q_{i2}, where 1 refers to manganese and 2 to sulfate.

The gas-phase species are SO_2, NH_3, H_2O and H_2SO_4. The ammonia and water concentrations are assumed uniform and constant. The SO_2 concentration decreases with distance due to plume dilution and conversion to H_2SO_4. The production of sulfuric acid vapor is described by (4). The droplet-phase concentrations of SO_2, NH_3 and H_2O are those in equilibrium with their prevailing gas-phase concentrations. Transport of sulfuric acid vapor to the par-

ticles occurs by diffusion, the mass transfer coefficient of which is given by (Fuchs and Sutugin, 1971)*

$$k_2 = \frac{2\pi D \mathscr{D}}{(1+\omega Kn)} \frac{M_{SO_4}}{RT}, \tag{5}$$

where $\omega = (1.333 + 0.71\,Kn^{-1})/(1 + Kn^{-1})$. $\overline{k}_{ij}$ and k_{ji} can be calculated from (A.33) and (A.34). The absorption of H_2SO_4 is irreversible, so $p_{j1e} = 0$.

An expression for the rate of the Mn-catalyzed oxidation of dissolved SO_2 to sulfate has been given by Wadden *et al.* (1974),

$$\frac{d[H_2SO_4]}{dt} = \frac{[MnSO_4](\alpha_1 y_{SO_2} - \alpha_2[H^+][HSO_4^-])}{\alpha_3 + y_{SO_2}}, \tag{6}$$

where [ ] represents concentrations in moles ℓ^{-1}, y is concentration in ppm, $\alpha_1 = 2.025\,\text{min}^{-1}$, $\alpha_2 = 4.254$ (moles $\ell^{-1})^{-2}$ (ppm min^{-1}), and $\alpha_3 = 200$ ppm. Converting (6) to the units used here, we have

$$R_2 = \frac{m_1 M_{SO_4}}{M_{Mn}}\left[\frac{\alpha_1 y_{SO_2} - \alpha_2[H^+][HSO_4^-]}{\alpha_3 + y_{SO_2}}\right]. \tag{7}$$

To obtain an expression for r_{2l}, we write (7) as $R_2 = r_{2l}M$. Assuming all particles in a section have the same composition, $m_1 = (Q_{l1}/Q_l)M$, from which

$$r_{2l} = \frac{Q_{l1}}{Q_l}\frac{M_{SO_4}}{M_{Mn}}\left[\frac{\alpha_1 y_{SO_2} - \alpha_2[H^+][HSO_4^-]}{\alpha_3 + y_{SO_2}}\right]. \tag{8}$$

The most involved aspect of the model application is the calculation of the sectional coagulation coefficients, ${}^1\overline{\beta}_{ijk}$ and ${}^2\overline{\beta}_{ij}$. Assuming the coagulation coefficient depends only on the volumes of the two particles, once the volumes of the particles are specified, ${}^1\overline{\beta}_{ijk}$ and ${}^2\overline{\beta}_{ik}$ can be determined from (A.34) and (A.35). In this work the Fuchs–Phillips expression for the Brownian coefficient $\beta(U, M)$ is used (Sitarski and Seinfeld, 1977). To calculate these coefficients it is necessary to relate the masses of Mn^{2+} and SO_4^{2-} to the volume of the particle. Relating the concentrations of manganese and sulfate to the size of the particle requires information on the complete particle composition that can be determined by imposing the condition that all species except Mn^{2+} and SO_4^{2-} be at their equilibrium concentrations.

The equilibrium computation is carried out as follows. At any time t', the total masses of manganese and sulfate, Q_{l1} and Q_{l2}, are known in each section l. A basic assumption of the approach is that all particles in a section have identical composition. Knowing Q_{l1} and Q_{l2}, we also know their ratio, Q_{l1}/Q_{l2}. The equilibrium constants required are given in Table 1. In the equilibrium calculation for each section there are three equations involving the three unknown quantities, I (ionic strength), $c_{SO_4^{2-}}$, and c_{H^+} (molalities of sulfate and H^+). (The molality of manganese can be used instead of that for sulfate since given the ratio Q_{l1}/Q_{l2}, only one of these two quantities is considered as unknown.) The three equations are those for the ionic strength, the water activity, and electroneutrality.

The ionic strength is related to the species molalities by (Denbigh, 1971)

$$I = \frac{1}{2}\sum_i c_i z_i^2, \tag{9}$$

where z_i is the charge on species i.

The water vapor equilibrium is expressed by (Stokes and Robinson, 1966)

$$1 = \sum \frac{c_i}{c_{bi}(a_w)}, \tag{10}$$

where c_{bi} is the molality of a binary solution of the i-th component and water at the same water activity a_w.

We assume that the effect of sulfite on water activity is the same as sulfate. Then, the droplet may be treated as a mixture of $MnSO_4$, $(NH_4)_2SO_4$ and H_2SO_4, and (10) may be solved for $\chi = c_{SO_4^{2-}} + c_{HSO_4^-} + c_{Mn^{2+}}$ as

$$\chi = \left[1 + \frac{1}{2}\left(\frac{1}{c_{bH_2SO_4}} - \frac{1}{c_{b(NH_4)_2SO_4}}\right)p_{NH_3}K_{hn}\left(a_w + \frac{K_{1a}c_{H^+}}{K_w}\right) - \frac{a_w}{c_{bH_2SO_4}}\left(p_{SO_2}K_{hs}\left(1 + \frac{K_{1s}}{\gamma_+\gamma_-c_{H^+}}\left(1 + \frac{K_{2s}\gamma_-}{\gamma_+\gamma_-c_{H^+}}\right)\right)\right)\right]\left[(1-\zeta)\left(\frac{1}{c_{bMnSO_4}} - \frac{1}{c_{bH_2SO_4}}\right) + \frac{\zeta}{c_{bH_2SO_4}}\right]^{-1}, \tag{11}$$

where $\zeta = (c_{SO_4^{2-}} + c_{HSO_4^-})/\chi$ and where the activity coefficients are approx. by (Davis, 1938)

$$\log \gamma_z = -\phi z^2\left(\frac{\sqrt{I}}{1+\sqrt{I}} - 0.2I\right). \tag{12}$$

γ_z is the activity coefficient for an ion with a charge z. For the system considered here $\phi = 0.5085$.

The condition of electroneutrality leads to

$$0 = -\frac{1}{c_{H^+}}\frac{a_w}{\gamma_+\gamma_-}\left[K_w + p_{SO_2}K_{hs}K_{1s}\right] - \frac{2p_{SO_2}K_{hs}K_{1s}K_{2s}a_w}{\gamma_+^2\gamma_{2-}c_{H^+}^2} + c_{H^+} + \frac{p_{NH_3}K_{hn}K_{1a}c_{H^+}}{K_w} + \chi\left[(2-4\zeta) + \frac{\gamma_{2-}\gamma_+\zeta c_{H^+}}{K_{4s}\gamma_- + \gamma_{2-}\gamma_+c_{H^+}}\right] \tag{13}$$

The ionic strength relation (9) can be written as

$$0 = 2I - \left[\frac{a_w}{\gamma_+\gamma_-c_{H^+}}(K_w + p_{SO_2}K_{hs}K_{1s}) + \frac{4p_{SO_2}K_{hs}K_{1s}K_{2s}a_w}{\gamma_+^2\gamma_{2-}c_{H^+}^2}\right.$$

* Since "component" 2 is sulfate, only the molecular weight of sulfate, M_{SO_4}, is needed in (5). The hydrogen atoms are automatically determined by the equilibrium calculation.

Table 1. Equilibrium constants for the aqueous SO_2-NH_3 system*

Reaction	Equilibrium constant†	Value @ 298 K
$H_2O \rightleftharpoons H^+ + OH^-$	$K_w = \frac{a_{H^+}a_{OH^-}}{a_w}$	1.008×10^{-14} (mol kg^{-1})^2
$SO_2(g) + H_2O \rightleftharpoons SO_2 \cdot H_2O$	$K_{h_1} = \frac{a_{SO_2 \cdot H_2O}}{p_{SO_2}a_w}$	1.231 mol kg^{-1} atm^{-1}
$SO_2 \cdot H_2O \rightleftharpoons H^+ + HSO_3^-$	$K_{1_1} = \frac{a_{H^+}a_{HSO_3^-}}{a_{SO_2 \cdot H_2O}}$	1.717×10^{-2} mol kg^{-1}
$HSO_3^- \rightleftharpoons H^+ + SO_3^{2-}$	$K_{2_1} = \frac{a_{H^+}a_{SO_3^{2-}}}{a_{HSO_3^-}}$	6.0139×10^{-9} mol kg^{-1}
$NH_3(g) + H_2O \rightleftharpoons NH_3 \cdot H_2O$	$K_{h_2} = \frac{a_{NH_3 \cdot H_2O}}{p_{NH_3}a_w}$	57.46 mol kg^{-1} atm^{-1}
$NH_3 \cdot H_2O \rightleftharpoons NH_4^+ + OH^-$	$K_{1_2} = \frac{a_{NH_4^+}a_{OH^-}}{a_{NH_3 \cdot H_2O}}$	1.798×10^{-5} mol kg^{-1}
$HSO_4^- \rightleftharpoons SO_4^{2-} + H^+$	$K_{d_1} = \frac{a_{H^+}a_{SO_4^{2-}}}{a_{HSO_4^-}}$	1.014×10^{-2} mol kg^{-1}

* Reference: Wagman *et al.* (1968)
† Water activity a_w = R.H./100, where R.H. is the relative humidity in %.

$$+\frac{p_{NH_3}K_{h_2}K_{1_2}c_{H^+}}{K_w} + c_{H^+} + \left(4 - \frac{3c_{H^+}\gamma_{2-}\gamma_{+}\zeta}{\gamma_{2-}\gamma_{+}c_{H^+} + K_{d_1}\gamma_{-}}\right)\chi\Bigg]. \quad (14)$$

Equations (13) and (14) may be solved iteratively as follows. First, values of c_{H^+} and I are assumed. Using the assumed value of I, the activity coefficients may be calculated from (12). The values of c_{H^+} and I are determined by iterating on (13) and (14).

The total mass of the particle is now available since the masses of Mn^{2+} and SO_4^{2-} are known together with their molalities. Finally, the volume of the particle can be calculated from

$$V = \frac{\left(\frac{10^3}{\rho_w} + \sum_i c_i v_i\right)M}{\zeta\chi M_{SO_4} + (1-\zeta)\chi M_{Mn}}, \quad (15)$$

where v_i is the molal volume of the i-th component. Values of v_i were calculated from data in International Critical Tables (1928), Klotz and Eckert (1942) and Lindstrom and Wirth (1969).

4. RESULTS OF PLUME SIMULATION

Figures 1–7 show the results of the calculations performed. In each figure the component mass concentrations are referred to the left-hand ordinate. The component mass concentrations are indicated by the shaded regions on each bar representing a section. The difference between the mass represented by the shaded regions and the total mass is that of water. In all cases, water comprises at least three-fifths of the mass of each section. Ten sections ($m = 10$) were used in the computations*. The sections were selected according to $D_0 = 0.01$ μm, $D_{10} = 5$ μm and $D_i/D_{i-1} = 1.86$.

* Results similar to those presented here were obtained using 20 sections.

Figure 1 shows the assumed "initial" size-composition distribution at 1 km. The "initial" distribution was chosen based on data reported by Eltgroth and Hobbs (1979) for the Centralia plume on 22 September, 1977 (entry (d) of Table 3 of that work). In addition, we have assumed that the initial plume aerosol consists of an aqueous solution of $MnSO_4$ in equilibrium with a relative humidity of 90%. This relative humidity was taken to be constant over the length of the plume. A uniform background concen-

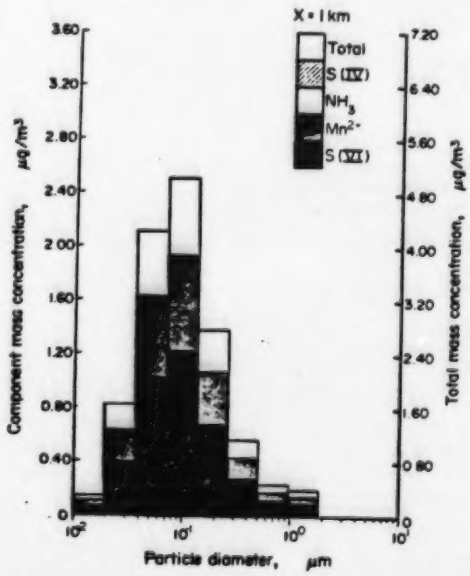

Fig. 1. Aerosol mass distribution at a distance of 1 km from the source. S(IV) refers to the total concentration of sulfur in oxidation state four, i.e. $SO_2 \cdot H_2O$, HSO_3^- and SO_3^{2-}. S(VI) refers to the total concentration of sulfur in oxidation state six, i.e. SO_4^{2-} and $HSO_4^- \cdot NH_3$ refers to the total concentration of $NH_3 \cdot H_2O$ and NH_4^+.

tration of NH_3 of 0.05 ppm was assumed. At 1 km, the concentration of SO_2 in the plume was taken to be 1.2 ppm. As the plume is diluted, the SO_2 concentration is reduced accordingly. (Sulfur dioxide is also depleted by gas-phase conversion to sulfuric acid and by absorption into the particles.)

Three cases were studied:

(i) Case 1 (Figs 2–3): no reactions, coagulation, dilution.

(ii) Case 2 (Figs 4–5): liquid-phase reaction only, coagulation, dilution.

(iii) Case 3 (Figs 6–7): all phenomena included; gas- and liquid-phase reactions, coagulation, dilution.

In each case, the size-composition distributions at 2 and 10 km downwind are shown. A common feature of each of the three cases is the depletion of the two lowest sections ($D_0 = 0.01\,\mu m$, $D_1 = 0.0186\,\mu m$, $D_2 = 0.0346\,\mu m$) due to coagulation with larger particles. Because we have not assumed that homogeneous nucleation is occurring, there is no source of fresh particles to replenish the two lower sections.

Case 1 shows the effects of coagulation and dilution on the size distribution. No reactions were assumed to be occurring. Section 4, centered around 0.1 μm dia., initially has the highest mass concentration. As the plume is carried downwind, dilution reduces the mass concentrations in all sections equally. Dilution is accounted for by the term $A^{-1}\,dA/dt'$. This term can be specified based on the conventional σ_y and σ_z parameters for the Gaussian plume equation. In this work, the Pasquill-Gifford (P–G) σ_y and σ_z parameters for neutral conditions were used. If the plume area A is taken as proportional to the product, $\sigma_y\sigma_z$, then

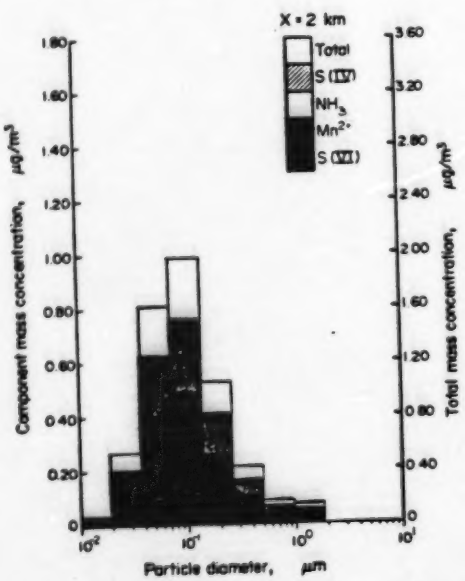

Fig. 2. Aerosol mass distribution at a distance of 2 km from the source resulting from coagulation and dilution of the distribution of Fig. 1.

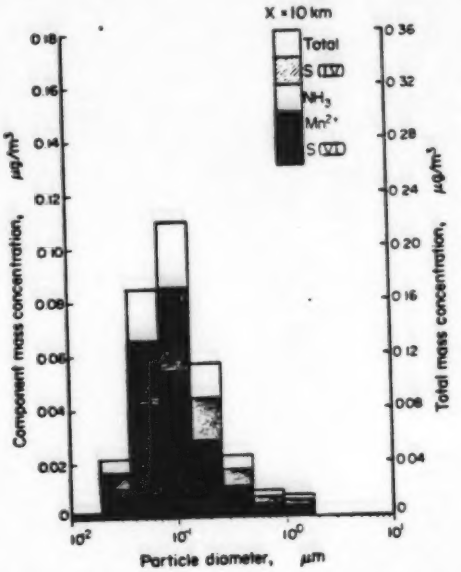

Fig. 3. Aerosol mass distribution at a distance of 10 km from the source resulting from coagulation and dilution of the distribution of Fig. 1.

$$\frac{1}{A}\frac{dA}{dt'} = \frac{1}{\sigma_y\sigma_z}\left[\sigma_y\frac{d\sigma_z}{dt'} + \sigma_z\frac{d\sigma_y}{dt'}\right]. \qquad (16)$$

Fitting functions of the form, $\sigma_y = a_y(t')^{b_y}$, and $\sigma_z = a_z(t')^{b_z}$, to the P–G neutral curves, we obtain

$$\frac{1}{A}\frac{dA}{dt'} = \frac{1.4}{t'}. \qquad (17)$$

From 1 to 10 km, the plume is diluted by a factor of 25.

The size distribution evolution in Figs 1–3 can be explained on the basis of the combined effects of dilution and coagulation. Particles in sections 1 and 2 are continually depleted through coagulation with those in higher sections. Conversely, the other sections gain mass by the same process. This effect is greatest for the smallest sections. For example, from 1 to 10 km, coagulation reduces the amount of mass in the first section by a factor of almost three. On the other hand, for the sixth section coagulation adds less than 1% of the final mass. Dilution simply lowers all concentrations equally whereas coagulation produces a shift toward the upper end of the spectrum.

Figures 4 and 5 show the mass distributions at 2 and 10 km when the manganese catalyzed liquid-phase oxidation of dissolved SO_2 is occurring, in addition to coagulation and dilution. In each section, the rate of formation of sulfate, expressed as a percentage of the total particle mass, depends only on the internal concentrations. Since the internal concentrations are initially equal for all sections, an equal percentage of the total mass of each section is added as sulfate with downwind distance. Thus, for example, at 2 km, the SO_4^{2-}, Mn^{2+}, NH_4^+, etc. fractions of the total mass of

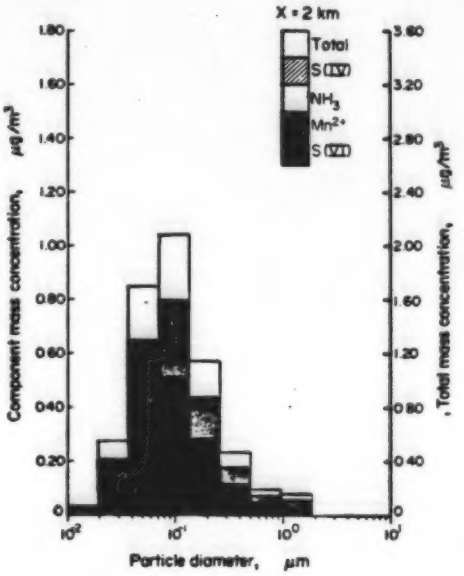

Fig. 4. Aerosol mass distribution at a distance of 2 km from the source resulting from coagulation, dilution, and liquid-phase oxidation of dissolved SO_2.

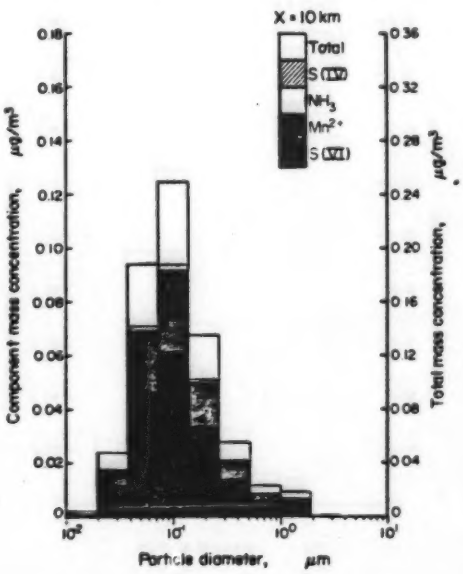

Fig. 5. Aerosol mass distribution at a distance of 10 km from the source resulting from coagulation, dilution, and liquid-phase oxidation of dissolved SO_2.

each section are equal. The values of these fractions change with downwind distance but remain uniform across the sections. At the rate of sulfate formation predicted by (7), the quantity of sulfate formed in each section is not large enough to alter substantially the total mass distributions from Case 1. For example, at

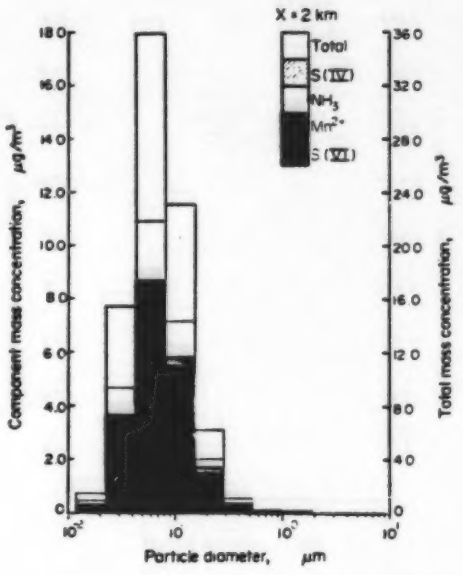

Fig. 6. Aerosol mass distribution at a distance of 2 km from the source resulting from coagulation, dilution, liquid-phase oxidation of dissolved SO_2, and gas-to-particle conversion of H_2SO_4 vapor formed by gas-phase oxidation of SO_2.

10 km, particles in Section 4 contain approximately 0.008 $\mu g\,m^{-3}$ of sulfate,* as compared to a total mass concentration in Section 4 of about 0.24 $\mu g\,m^{-3}$.

Case 3 (Figs. 6 and 7) includes all the phenomena of interest. Gas-phase oxidation of SO_2 to H_2SO_4 is now assumed to occur, with a first-order rate constant $k_g = 0.05\,h^{-1}$. The sulfuric acid vapor is absorbed by the particles, directly contributing sulfate to that being formed in the liquid-phase by the manganese catalyzed oxidation. We note that for the specific parameters of our study, this gas-phase oxidation rate dominates that in the liquid phase. For example, at 10 km, particles in Section 4 contain about 10 $\mu g\,m^{-3}$ of sulfate, as compared with about 0.008 $\mu g\,m^{-3}$ in the previous case. Because of the hygroscopicity of sulfate, a large amount of water is associated with the particles. Thus, the total mass concentration of particles in Section 4 in this case is about 40 $\mu g\,m^{-3}$, as compared with 0.24 $\mu g\,m^{-3}$ in Case 2. When the sulfate is being added by gas-to-particle conversion, more sulfate per unit mass is added to the smaller particles.

Recall that sections are defined in terms of M, the total mass of metal and sulfate, rather than in terms of particle diameter. Thus, as the composition of a section changes, its boundaries, expressed in terms of particle diameter may change. This happens in Fig. 6. From 1 km to 2 km a large amount of sulfate from the gas phase is deposited on the drop. Thus, the main

* This sulfate refers to that formed by reaction beyond that present initially as $MnSO_4$.

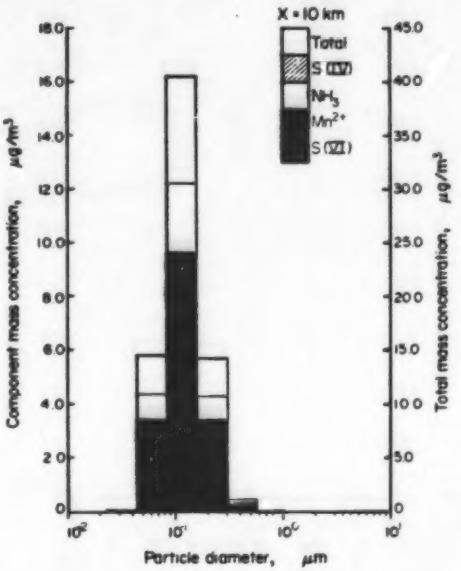

Fig. 7. Aerosol mass distribution at a distance of 10 km from the source resulting from coagulation, dilution, liquid-phase oxidation of dissolved SO_2, and gas-to-particle conversion of H_2SO_4 vapor formed by gas-phase oxidation of SO_2.

component changes from $MnSO_4$ to $(NH_4)_2SO_4$. As a result of this change, for a given amount of metal plus sulfate, the droplet has a larger diameter. Note, for example, that the lower boundary of the first section becomes larger than 0.01 μm.

The ratio of sulfate added to the particles by gas-to-particle conversion to that produced by heterogeneous reaction decreases as particle diameter increases. Thus, even though on an overall basis, for the particular set of parameters chosen here, the gas-phase oxidation of SO_2 is more important than that in the liquid phase, internal reaction dominates the rate of sulfate production in large particles.

The rate of liquid-phase sulfate formation is second-order overall, being proportional to the product, $y_{SO_2}Q_i$. (If y_{SO_2} greatly exceeds 200 ppm, the value of α_3 in the rate expression (6), the rate becomes independent of y_{SO_2}. In the situation considered here, SO_2 concentrations are well below this value.) On the other hand, the homogeneous conversion of SO_2 to H_2SO_4 is first-order. As the plume is diluted, the rate of the heterogeneous reaction is quenched relative to that of the first-order reaction, a phenomenon that has been discussed in detail by Freiberg (1978) and Schwartz and Newman (1978). As a result, the particle size at which homogeneous and heterogeneous sulfate production mechanisms are roughly equal increases with downwind distance.

5. CONCLUSIONS

A model for computing the size-composition distribution of plume aerosols has been presented and applied to a hypothetical, yet realistic, example of a power plant plume aerosol. The evolution of the aerosol size and composition distribution averaged across the plume has been calculated as a function of down wind distance. Upon emission, the aerosol was assumed to consist of aqueous droplets of $MnSO_4$. During transport downwind and dilution, the plume particles interact by coagulation and grow due to liquid-phase catalytic oxidation of dissolved SO_2 and gas-to-particle conversion of sulfuric acid vapor formed by the gas-phase oxidation of SO_2. Based on the work of Gelbard and Seinfeld (1980), the model consists of a set of ordinary differential equations for Q_{li}, the mass of component i in section l, where the aerosol size spectrum has been segmented into m sections ($l = 1, 2, \ldots, m$). The set of ordinary differential equations is solved by standard methods. The model presented in this work has the unique capability of simulating both the aerosol size and composition distributions and therefore can be used as an aerosol dynamics component of detailed plume models.

Acknowledgement—This work was supported by U.S. Environmental Protection Agency grant R806844. The research reported in this paper made use of computational facilities funded through grants from the Camille and Henry Dreyfus Foundation and the National Science Foundation (Grant No. CHE78-20235). Fred Gelbard was supported by NIEHS grant 5P30-ES02109-03 under the Center for Health Effects of Fossil Fuels Utilization of the Harvard—MIT Division of Health Sciences and Technology and the Energy Laboratory.

REFERENCES

Davies C. W. (1938) The extent of dissociation of salts in water. Part VIII. *J. chem. Soc.* 2093–2098.

Denbigh K. (1971) *The Principles of Chemical Equilibrium*, Cambridge University Press, Cambridge, pp. 312.

Eltgroth M. W. and Hobbs P. V. (1979) Evolution of particles in the plumes of coal-fired power plants—II. A numerical model and comparisons with field measurements. *Atmospheric Environment* 13, 953–976.

Freiberg J. (1978) Conversion limit and characteristic time of SO_2 oxidation in plumes. *Atmospheric Environment* 12, 339–347.

Fuchs N. A. and Sutugin A. G. (1971) High dispersed aerosols. In *Topics in Current Aerosol Research* Vol. 2, p. 35. (Edited by G. M. Hidy and J. R. Brock). Pergamon Press, Oxford.

Gelbard F. and Seinfeld J. H. (1980) Simulation of multicomponent aerosol dynamics. *J. Colloid Interface Sci.* 78, 485–501.

Hidy G. M. (1975) Summary of the California Aerosol Characterization Experiment. *J. Air Pollut. Control Ass.* 25, 1106–1114.

International Critical Tables (1928) First Edition, 3, 56, 60, 68.

Klotz J. M. and Eckert C. F. (1942) The apparent molal volumes of aqueous solutions of sulfuric acid at 25°. *J. Am. chem. Soc.* 64, 1878–1880.

Lindstrom R. E. and Wirth H. E. (1969) Estimation of the bisulfate ion dissociation in solutions of sulfuric acid and sodium bisulfate. *J. phys. Chem.* 73, 218–223.

Schwartz S. E. and Newman L. (1978) Processes limiting the oxidation of sulfur dioxide in stack plumes. *Envir. Sci. Technol.* 12, 67–73.

Seinfeld J. H. and Ramabhadran T. E. (1975) Atmospheric aerosol growth by heterogeneous condensation. *Atmospheric Environment* 9, 1091–1097.

Sitarski M. and Seinfeld J. H. (1977) Brownian coagulation in the transition regime. *J. Colloid Interface Science* **61**, 261–271.

Stokes R. H. and Robinson R. A. (1966) Interactions in aqueous nonelectrolyte solutions. I. Solute-solvent equilibria. *J. phys. chem.* **70**, 2126–2131.

Wadden R. A., Quon J. E. and Hulburt H. M. (1974) A model of a growing coagulating aerosol. *Atmospheric Environment* **8**, 1009–1028.

Wagman D. D. *et al.* (1968) Selected values of chemical thermodynamic properties. NBS Technical Note 270–3.

Whitby K. T. (1978) The physical characteristics of sulfur aerosols. *Atmospheric Environment* **12**, 135–139.

Willeke K. and Whitby K. T. (1975) Atmospheric aerosols: size distribution interpretation. *J. Air Pollution Control Ass.* **25**, 529–534.

Willeke K., Whitby K. T., Clark W. E. and Marple V. A. (1974) Size distributions of Denver aerosols—A comparison of two sites. *Atmospheric Environment* **8**, 609–633.

APPENDIX A1: MODEL DEVELOPMENT

Derivation of the equation governing the mean aerosol size-composition distribution function in a plume from a continuous point source

Let M denote the total mass of a particle. Let m_i be the mass of the i-th component in the particle. Let $\mathbf{m} = (m_1, \ldots, m_{s-1})$, where the particle has s components. Note that m_s has been omitted from the $\mathbf{m}$ vector, because it is fixed once the rest of the m_i's are given, i.e.,

$$\sum_{i=1}^{s} m_i = M. \tag{A.1}$$

Then, let $n(\mathbf{m}, M, \mathbf{x}, t)\, dm_1 \ldots dm_{s-1}\, dM$ be the number of particles having total mass M in the range $[M, M+dM]$, mass of component i, m_i in the range $[m_i, m_i + dm_i]$, $i = 1, 2, \ldots, s-1$, at location $\mathbf{x}$ at time t. The rate of change of n is

$$\left.\frac{\partial n}{\partial t}\right|_{\text{total}} = \left.\frac{\partial n}{\partial t}\right|_{\text{drifting}} + \left.\frac{\partial n}{\partial t}\right|_{\text{coagulation}} + \left.\frac{\partial n}{\partial t}\right|_{\text{sources}} + \left.\frac{\partial n}{\partial t}\right|_{\text{Brownian diffusion}} \tag{A.2}$$

Using the divergence theorem in $s+3$ dimensions, the drifting term is

$$\left.\frac{\partial n}{\partial t}\right|_{\text{drifting}} = -\hat{\nabla}\cdot(n\hat{\mathbf{u}}), \tag{A.3}$$

where

$$\hat{\nabla} = \left[\frac{\partial}{\partial m_1}, \frac{\partial}{\partial m_2}, \ldots \frac{\partial}{\partial m_{s-1}}, \frac{\partial}{\partial M}, \frac{\partial}{\partial x_1}, \frac{\partial}{\partial x_2}, \frac{\partial}{\partial x_3}\right],$$

$$\hat{\mathbf{u}} = \left[\frac{\partial m_1}{\partial t}, \frac{\partial m_2}{\partial t}, \ldots \frac{\partial m_{s-1}}{\partial t}, \frac{\partial M}{\partial t}, u_1, u_2, u_3 - w_s\right].$$

Here, $\mathbf{u} = (u_1, u_2, u_3)$ is the velocity of the air and $w_s = w_s(M)$ is the settling velocity.

Let $R_i(\mathbf{m}, M)$ and $I_i(\mathbf{m}, M, \mathbf{x}, t)$ represent the net rate of change of component i in a particle due to intra-particle chemical reaction and condensation, respectively. Note that I_i is the rate of condensation minus that of evaporation. Then

$$\frac{\partial m_i}{\partial t} = I_i + R_i, \tag{A.4}$$

and

$$\frac{\partial M}{\partial t} = I_T + R_T, \tag{A.5}$$

where

$$I_T = \sum_{i=1}^{s} I_i, \tag{A.6}$$

$$R_T = \sum_{i=1}^{s} R_i. \tag{A.7}$$

The coagulation term in (A.2) may be written as

$$\left.\frac{\partial n}{\partial t}\right|_{\text{coagulation}} = \frac{1}{2}\int_0^M \int_0^\infty \cdots \int_0^\infty \beta(U, M-U) n(\boldsymbol{\zeta}, U, \mathbf{x}, t) \times n(\mathbf{m}-\boldsymbol{\zeta}, M-U, \mathbf{x}, t)\, d\boldsymbol{\zeta}\, dU - \int_0^\infty \cdots \int_0^\infty \beta(U, M) n(\boldsymbol{\zeta}, U, \mathbf{x}, t) \times n(\mathbf{m}, M, \mathbf{x}, t)\, d\boldsymbol{\zeta}\, dU, \tag{A.8}$$

where $\beta(U, M)$ is the coagulation coefficient for particles with masses U and M. Note that $n(\mathbf{m}, U, \mathbf{x}, t) = 0$ if

$$U < \sum_{i=1}^{s-1} m_i.$$

Because of this condition, the limits on the integrals in (A.8) can be extended from $-\infty$ to ∞ as n is zero whenever any of the m_i's are negative.

The Brownian diffusion term in (A.2) is given by

$$\left.\frac{\partial n}{\partial t}\right|_{\substack{\text{Brownian}\\ \text{diffusion}}} = \mathcal{D}_B \sum_{i=1}^{3} \frac{\partial^2 n}{\partial x_i^2}, \tag{A.9}$$

where $\mathcal{D}_B$ is the Brownian diffusivity. However, transport by Brownian diffusion is negligible compared with that of turbulent diffusion, and this term can be neglected. Finally, let $S(\mathbf{m}, M, \mathbf{x}, t)$ represent the source term in (A.2).

We now time average (A.2) and use an overbar to denote the average values. Let $C[n, n]$ denote the coagulation term of (A.8). Time averaging gives

$$\frac{\partial \bar{n}}{\partial t} = -\sum_{i=1}^{s-1} \frac{\partial}{\partial m_i}\left(\bar{I}_i \bar{n} + \overline{I_i' n'} + R_i \bar{n}\right) - \frac{\partial}{\partial M}\left[\sum_{i=1}^{s}\left(\bar{I}_i \bar{n} + \overline{I_i' n'} + R_i \bar{n}\right)\right] - \sum_{i=1}^{3} \frac{\partial}{\partial x_i}\left(\bar{u}_i \bar{n} + \overline{u_i' n'}\right) + C[\bar{n}, \bar{n}] + \overline{C[n', n']} + \bar{S} + \frac{\partial}{\partial x_3} w_s \bar{n}. \tag{A.10}$$

In general, I_i can be expressed as

$$I_i = k_i(M)(p_i - p_{iw}), \tag{A.11}$$

where $k_i(M)$ is a mass transfer coefficient, $p_i = p_i(\mathbf{x}, t)$ is the partial pressure of species i in the bulk fluid, and p_{iw} is the partial pressure of i just above the particle surface in equilibrium with that in the droplet.

We will assume that the stochastic coagulation term is small compared to the mean coagulation rate,

$$C[\bar{n}, \bar{n}] \gg \overline{C[n', n']},$$

and that the turbulent species fluxes can be represented by eddy diffusivities,

$$\frac{\partial}{\partial x_i}\overline{u_i' n'} = -K_u \frac{\partial \bar{n}}{\partial x_i}.$$

Seinfeld and Ramabhadran (1975) considered the stochastic condensation term, $\overline{I_i' n'}$, and showed that this term is generally negligible compared with $\bar{I}_i \bar{n}$, and it will henceforth be neglected here.

Using these assumptions in (A.10) gives

$$\frac{\partial \bar{n}}{\partial t} = -\sum_{i=1}^{s-1} \frac{\partial}{\partial m_i}\left[k_i(M)(\bar{p}_i - p_{iw})\bar{n} + R_i \bar{n}\right] - \frac{\partial}{\partial M}\left[\sum_{i=1}^{s}\left(k_i(M)(\bar{p}_i - p_{iw})\bar{n} + R_i \bar{n}\right)\right] - \sum_{i=1}^{3} \frac{\partial}{\partial x_i}\left(\bar{u}_i \bar{n} - K_u \frac{\partial \bar{n}}{\partial x_i}\right) + C[\bar{n}, \bar{n}] + \bar{S} + \frac{\partial}{\partial x_3} w_s \bar{n}. \tag{A.12}$$

This is the general equation governing the mean aerosol size-composition density function in the atmosphere.

We wish to apply this equation to typical plume geometries. Define the plume cross-sectional averages,

$$\langle \bar{p}_i \rangle = \frac{1}{A}\int\int \bar{p}_i(x_1, x_2, x_3)\,dx_2 dx_3, \quad (A.13)$$

$$\langle \pi \rangle = \frac{1}{A}\int\int \pi(\mathbf{m}, M, \mathbf{x}, t)\,dx_2 dx_3, \quad (A.14)$$

where $A = A(x_1)$ is the cross-sectional area of the plume at downwind distance x_1.

We now average (A.12) across the cross-section of the plume. In general, R_i will be independent of $\mathbf{x}$ so

$$\frac{1}{A}\int\int R_i \pi\,dx_2 dx_3 = R_i \langle \pi \rangle. \quad (A.15)$$

It will be assumed that*

$$\frac{1}{A}\int\int \bar{p}_i \pi\,dx_2 dx_3 = \langle \bar{p}_i \rangle \langle \pi \rangle. \quad (A.16)$$

Consider next the advection term. Assume that both $\bar{u}_2$ and $\bar{u}_3$ are zero. Further, assume that $\bar{u}_1$ is constant across the plume. The advection term becomes

$$\bar{u}_1 \frac{1}{A}\frac{\partial}{\partial x_1}\int\int \pi\,dx_2 dx_3 = \left(\bar{u}_1 \frac{\partial}{\partial x_1}\langle \pi \rangle\right) + \bar{u}_1 \langle \pi \rangle \frac{1}{A}\frac{dA}{dx_1}. \quad (A.17)$$

Next, we consider the turbulent diffusion term. It is customary to neglect the x_1-term (the "slender plume approximation"). Choose the region of integration so that the gradients of $\langle \pi \rangle$ vanish at the boundaries. Thus, the entire turbulent diffusion term vanishes from the spatially averaged equation.

For the coagulation term, assume that†

$$\langle C[\pi, \pi] \rangle = C[\langle \pi \rangle, \langle \pi \rangle]. \quad (A.18)$$

Let $\langle \bar{S} \rangle$ represent the cross sectional average of the source term and neglect the settling term (restricting our analysis to aerosols of dia. 1 μm and smaller.)

We are interested in steady state conditions. However, in the case of a plume, x_1 and "time" are related, so we can define a new "time" variable, $t' = x_1/\bar{u}_1$. Note that t' is the time a parcel of fluid has been in the plume.

Thus, (A.12) becomes for a continuous plume,

$$\frac{\partial \langle \pi \rangle}{\partial t'} = -\sum_{i=1}^{s-1}\frac{\partial}{\partial m_i}\left[k_i(M)\left(\langle \bar{p}_i \rangle - p_{iw}\right)\langle \pi \rangle + R_i \langle \pi \rangle\right] - \frac{\partial}{\partial M}\left[\sum_{i=1}^{s}\left\{k_i(M)\left(\langle \bar{p}_i \rangle - p_{iw}\right)\langle \pi \rangle + R_i \langle \pi \rangle\right\}\right] - \langle \pi \rangle \frac{1}{A}\frac{dA}{dt'} + C[\langle \pi \rangle, \langle \pi \rangle] + \langle \bar{S} \rangle. \quad (A.19)$$

* The error introduced by this assumption can be estimated by assuming Gaussian profiles for both p and n. The fractional error is defined as $\varepsilon = \langle \bar{p}_i \pi \rangle - \langle \bar{p}_i \rangle \langle \pi \rangle / \langle \bar{p}_i \pi \rangle$. If the area A is selected to include 75% of the plume mass, $\varepsilon = 0.13$. If A is chosen to include 80% of the plume mass, $\varepsilon = 0.17$.

† The error introduced by this assumption can be estimated from a typical plume cross-sectional profile for total aerosol number density, $N(\text{cm}^{-3})$. The fractional error is given by $\varepsilon = (\langle N^2 \rangle - \langle N \rangle \langle N \rangle / \langle N^2 \rangle)$. For example, using the distribution from Fig. 19 of Eltgroth and Hobbs (1979), ε was found to be 0.07.

APPENDIX A.2: DERIVATION OF THE SECTIONAL EQUATIONS

The numerical solution of (A.19) poses a difficult problem. If the size spectrum is divided into a set of sections, over each of which the particle composition is assumed to be uniform, then (A.19) can be converted to a set of ordinary differential equations that are easy to solve and implement.

To sectionalize (A.19), multiply (A.19) by m_i and integrate over M from M_{l-1} to M_l and over all $\mathbf{m}$. Let‡

$$Q_{li} = \int_{M_{l-1}}^{M_l}\int_{-\infty}^{\infty}\cdots\int_{-\infty}^{\infty} m_i \langle \pi \rangle\,d\mathbf{m}\,dM, \quad (A.20)$$

$$Q_l = \int_{M_{l-1}}^{M_l}\int_{-\infty}^{\infty}\cdots\int_{-\infty}^{\infty} M \langle \pi \rangle\,d\mathbf{m}\,dM, \quad (A.21)$$

$$\langle \bar{S}_{li} \rangle = \int_{M_{l-1}}^{M_l}\int_{-\infty}^{\infty}\cdots\int_{-\infty}^{\infty} m_i \langle \bar{S} \rangle\,d\mathbf{m}\,dM. \quad (A.22)$$

Consider the first term of (A.19). After multiplying by m_i and integrating, it is of the form

$$\int_{M_{l-1}}^{M_l}\int_{-\infty}^{\infty}\cdots\int_{-\infty}^{\infty} m_i \frac{\partial}{\partial m_j} f_j\,d\mathbf{m}\,dM = \begin{cases} 0 & i \neq j \\ -\int_{M_{l-1}}^{M_l}\int_{-\infty}^{\infty}\cdots\int_{-\infty}^{\infty} f_i\,d\mathbf{m}\,dM & i = j. \end{cases} \quad (A.23)$$

Similarly, the second summation becomes

$$\int_{-\infty}^{\infty}\cdots\int_{-\infty}^{\infty} m_i \sum_{j=1}^{s}\left(k_j(M)(\langle \bar{p}_j \rangle - p_{jw})\langle \pi \rangle + R_i \langle \pi \rangle\right)d\mathbf{m}\Big|_{M_{l-1}}^{M_l}. \quad (A.24)$$

Consider the coagulation term $C[\langle \pi \rangle, \langle \pi \rangle]$,

$$\int_{M_{l-1}}^{M_l}\int_{-\infty}^{\infty}\cdots\int_{-\infty}^{\infty} m_i C[\langle \pi \rangle, \langle \pi \rangle]\,d\mathbf{m}\,dM = \frac{1}{2}\int_{-\infty}^{\infty}\cdots\int_{-\infty}^{\infty} m_i \beta(U, M-U) \langle \pi(\mathbf{m}-\xi, M-U, t') \rangle \times \langle \pi(\xi, U, t') \rangle\,d\xi\,d\mathbf{m}\,dU\,dM + \int_{M_{l-1}}^{M_l}\int_{0}^{\infty}\int_{-\infty}^{\infty}\cdots\int_{-\infty}^{\infty} m_i \beta(U, M) \langle \pi(\xi, U) \rangle \langle \pi(\mathbf{m}, M) \rangle\,d\xi\,d\mathbf{m}\,dU\,dM. \quad (A.25)$$

In the first integral, change variables. Let $\zeta = \mathbf{m} - \xi$ and $W = M - U$. Introduce the function defined by

$$\theta(\text{condition}) = \begin{cases} 1 & \text{if the condition is true} \\ 0 & \text{otherwise.} \end{cases}$$

With the above substitutions, (A.19) becomes

$$\frac{dQ_{li}}{dt'} = \int_{M_{l-1}}^{M_l}\int_{-\infty}^{\infty}\cdots\int_{-\infty}^{\infty}\left[k_i(M)(\langle \bar{p}_i \rangle - p_{iw})\langle \pi \rangle + R_i \langle \pi \rangle\right]d\mathbf{m}\,dM - \int_{-\infty}^{\infty}\cdots\int_{-\infty}^{\infty} m_i \sum_{j=1}^{s}\left[k_j(M) \times (\langle \bar{p}_j \rangle - p_{jw})\langle \pi \rangle + R_j \langle \pi \rangle\right]d\mathbf{m}\Big|_{M_{l-1}}^{M_l} + \frac{1}{2}\sum_{j=1}^{l}\sum_{k=1}^{l}\int_{M_{j-1}}^{M_j}\int_{M_{k-1}}^{M_k}$$

‡ Notational consistency would dictate that Q_{li} be written as $\langle \bar{Q}_{li} \rangle$, denoting both temporal and spatial averaging. For simplicity, we neglect the overbar and brackets on Q_{li} and Q_l.

$$\times \int_{-\infty}^{\infty} \cdots \int_{-\infty}^{\infty} (\zeta_i + \xi_i)\beta(U, W)\theta$$
$$\times (M_{l-1} < U + W < M_l)$$
$$\cdot \langle n(U, \xi, t')\rangle \langle n(W, \zeta, t')\rangle \, d\xi \, d\zeta \, dW dU$$
$$- \sum_{j=1}^{\infty} \int_{M_{l-1}}^{M_l} \int_{M_{j-1}}^{M_j} \int_{-\infty}^{\infty} \cdots \int_{-\infty}^{\infty} m_i \beta(U, M)$$
$$\times \langle n(\xi, U, t')\rangle \langle n(m, M, t')\rangle \, d\xi \, dm \, dU \, dM$$
$$- Q_{li} \frac{1}{A} \frac{dA}{dt'} + \langle \bar{S}_{li} \rangle. \quad \text{(A.26)}$$

In the above equation, the first term on the right represents the total mass of i added to particles within the section by condensation and reaction. The second term represents the change in i due to growth into or out of section l.

In order to put (A.26) into closed form, it is necessary to know the behavior of $\langle n(M, m)\rangle$ as a function of M. Unfortunately, the only quantity that is known in a given section is the average value of $\langle n\rangle$ in that section. Since particle mass, rather than the number of particles, is conserved, it will be assumed that particle mass, not number, is uniformly distributed. In addition, since experimental data are usually plotted against the logarithm of particle diameter, it will be assumed that particle mass in a section is evenly distributed in terms of the logarithm of diameter. The curve for the actual mass distribution is approximated by a horizontal line, $M(dN/d\log D) = q_l(t)$*, in each section, where $q_l(t)$ is the average mass concentration in the section. In terms of $\langle n\rangle$, this becomes

$$M \langle n(M, m)\rangle = q_l(t) \frac{d}{dM} \log D. \quad \text{(A.27)}$$

Using (A.27) in (A.21) gives

$$Q_l(t) = q_l(t) \log \frac{D_l}{D_{l-1}}, \quad \text{(A.28)}$$

where D_l is the particle diameter corresponding to M_l. Using (A.27) in (A.28) gives

$$\langle n(m, M)\rangle = \frac{Q_l}{M^2 \Delta_l}, \quad \text{(A.29)}$$

where $\Delta_l = \ln \dfrac{M_l}{M_{l-1}}$.

* Througout this paper, $\log D$ is used as a shorthand notation for $\log(D/1\ \mu m)$.

Assuming that the composition of all particles within a section is uniform, we have

$$\int_{M_{l-1}}^{M_l} \int_{-\infty}^{\infty} \cdots \int_{-\infty}^{\infty} k_j(M) p_{lu} \langle n\rangle \, dm \, dM = p_{lu}$$
$$\times \int_{M_{l-1}}^{M_l} \int_{-\infty}^{\infty} \cdots \int_{-\infty}^{\infty} k_j(M) \langle n\rangle \, dm \, dM. \quad \text{(A.30)}$$

where p_{lu} is the value of p_{ju} evaluated at the mean particle mass and composition of section l. We express the rate of heterogeneous reaction R_i as $r_{li}M$ in evaluating the second term in the integrand of (A.26).

The second term in (A.26) is to be evaluated between the upper and lower limits of the l-th section. There is some ambiguity about how the values at the limits related to the Q_{li}, which are averages over the entire section. As mentioned previously, this term represents the effect of particles growing into the next larger section. This rate will be determined by the conditions in the section the particles are leaving. Thus, the upper and lower limits of this term will be evaluated using quantities in the l-th and $(l-1)$-th sections, respectively.

With these assumptions, (A.26) becomes

$$\frac{dQ_{li}}{dt'} = [\bar{k}_{li}(\bar{p}_l - p_{lu}) + r_{li}] Q_l$$
$$- \left[\sum_{j=1}^{i} \left(k_{lj}(\langle p_i\rangle - p_{lu}) + r_{lj}\Delta_l^{-1} \right) Q_{ji} \right]_{p=l-1}^{p=l}$$
$$+ \frac{1}{2} \sum_{j=1}^{i} \sum_{k=1}^{i} ({}^{2}\bar{p}_{jk} Q_{ji} Q_{ki} + {}^{2}\bar{p}_{kj} Q_{ki} Q_j)$$
$$- Q_{li} \sum_{j=1}^{\infty} {}^{2}\bar{p}_{lj} Q_j - Q_{li} \frac{1}{A} \frac{dA}{dt'} + \langle \bar{S}_{li}\rangle, \quad \text{(A.31)}$$

where

$$\bar{k}_{li} = \int_{M_{l-1}}^{M_l} \frac{k_i(M)}{M^2 \Delta_l} dM, \quad \text{(A.32)}$$

$$k_{lj} = \frac{k_j(M_q)}{M \Delta_q}, \quad \text{(A.33)}$$

$${}^{2}\bar{p}_{jk} = \int_{M_{j-1}}^{M_j} \int_{M_{k-1}}^{M_k} \frac{\beta(U, M)\theta(M_{l-1} < U + M \leq M_l)}{U^2 M \Delta_j \Delta_k} dU \, dM, \quad \text{(A.34)}$$

$${}^{2}\bar{p}_{lu} = \int_{M_{l-1}}^{M_l} \int_{M_{j-1}}^{M_j} \frac{\beta(U, M)}{U^2 M \Delta_l \Delta_j} dU \, dM. \quad \text{(A.35)}$$